The Journal of Physiology

Maternal obesity epigenetically alters visceral fat progenitor cell properties in male offspring mice

Xingwei Liang[1], Qiyuan Yang[1], Xing Fu[1], Carl J. Rogers[1], Bo Wang[1], Hong Pan[1], Mei-Jun Zhu[3], Peter W. Nathanielsz[4] and Min Du[1,2]

[1] *Washington Centre for Muscle Biology and Department of Animal Sciences, Washington State University, Pullman, WA, USA*
[2] *Beijing Advanced Innovation Centre for Food Nutrition and Human Health, College of Food Science & Nutritional Engineering, China Agricultural University, Beijing, China*
[3] *School of Food Sciences, Washington State University, Pullman, WA, USA*
[4] *Wyoming Pregnancy and Life Course Health Centre, Department of Animal Science, University of Wyoming, Laramie, Wyoming, USA*

Key points

- Maternal obesity reduces adipogenic progenitor density in offspring adipose tissue.
- The ability of adipose tissue expansion in the offspring of obese mothers is limited and is associated with metabolic dysfunction of adipose tissue when challenged with a high-fat diet.
- Maternal obesity induces DNA demethylation in the promoter of zinc finger protein 423, which renders progenitor cells with a high adipogenic capacity.
- Maternal obesity demonstrates long-term effects on the adipogenic capacity of progenitor cells in offspring adipose tissue, demonstrating a developmental programming effect.

Abstract Maternal obesity (MO) programs offspring obesity and metabolic disorders, although the underlying mechanisms remain poorly defined. Progenitor cells are the source of new adipocytes. The present study aimed to test whether MO epigenetically predisposes adipocyte progenitors in the fat of offspring to adipogenic differentiation and subsequent depletion, which leads to a failure of adipose tissue plasticity under positive energy balance, contributing to adipose tissue metabolic dysfunction. C57BL/6 female mice were fed either a control diet (10% energy from fat) or a high-fat diet (45% energy from fat) for 8 weeks before mating. Male offspring of control (Con) and obese (OB) dams were weaned onto a regular (Reg) or obesogenic (Obe) diet until 3 months of age. At weaning, male OB offspring had a higher expression of Zinc finger protein 423 (*zfp423*), a key transcription factor in adipogenesis, as well as lower DNA methylation of its promoter in progenitors of epididymal fat compared to Con offspring, which was correlated with enhanced adipogenic differentiation. At 3 months of age, progenitor density was 30.9 $\pm$ 9.7% lower in OB/Obe compared to Con/Obe mice, accompanied by a limited expansion of the adipocyte number when challenged with a high-energy diet. This difference was associated with lower DNA methylation in the *zfp423* promoter in the epididymal fat of OB/Obe offspring, which was correlated with greater macrophage chemotactic protein-1 and hypoxia-inducible factor 1α expression. In summary, MO epigenetically limits the expansion capacity of offspring adipose tissue, providing an explanation for the adipose metabolic dysfunction of male offspring in the setting of MO.

(Received 6 January 2016; accepted after revision 29 March 2016; first published online 6 April 2016)
Corresponding author M. Du: Washington Centre for Muscle Biology, Department of Animal Sciences, Washington State University, Pullman, WA 99164, USA. Email: min.du@wsu.edu

Abbreviations aP2, adipocyte protein 2; EpiWAT, epididymal white adipose tissue; H&E, haemotoxylin and eosin; IL-6, interleukin-6; IngWAT, inguinal white adipose tissue; MCP, macrophage chemotactic protein; MO, maternal obesity; PDGFRα, plate-derived growth factor receptor α; Pref1, preadipocyte factor 1; PPARγ, peroxisome proliferator-activated receptor γ; SVFs, stromal-vascular fractions; TNF, tumor necrosis factor; *zfp423*, zinc finger protein 423.

DOI: 10.1113/JP272123

Introduction

According to the latest NHANES (National Health and Nutrition Examination Survey) in 2009 to 2010, 31.9% of non-pregnant women of childbearing age (aged 20–39 years) in the USA are obese, and another one-third are overweight (Flegal *et al.* 2012). In addition, there is a shift towards higher gestational weight gain, reflecting the prevalence of excessive nutrient intake during gestation in affluent countries (Waters *et al.* 2012). Maternal obesity (MO) in combination with an obesogenic diet can program harmful, persistent metabolic dysfunction in offspring, including pre-disposition to obesity and type 2 diabetes mellitus (Blackmore *et al.* 2014; Desai *et al.* 2015; Patel *et al.* 2015). Obesity now affects 17% of children in the USA, tripling the rate from just one generation ago (Ogden *et al.* 2010), and is accompanied by increased rates of childhood metabolic diseases (Biro & Wien, 2010; Shasa *et al.* 2015). The causative mechanisms for this maternal programming influence on offspring remain poorly defined.

Major adipose tissue development occurs between late gestation to 4 weeks of postnatal age in rodents (Greenwood & Hirsch, 1974), although, to some extent, adipose tissue of both humans and rodents remains expandable later in life (Greenwood & Hirsch, 1974; Spalding *et al.* 2008). Adipocyte hyperplasia largely ceases at adolescence (Spalding *et al.* 2008). Thus, the major development of adipose tissue coincides with plastic periods of pregnancy and lactation, when MO probably programs permanent changes in properties of offspring adipose tissue. In agreement with this concept, previous studies have shown that maternal adiposity correlates with offspring adiposity in rodents (Shankar *et al.* 2008) and human neonates (Modi *et al.* 2011).

White adipocytes are derived from platelet-derived growth factor receptor α (PDGFRα) positive cells, which are the putative progenitors for adipogenesis (Lee & Granneman, 2012; Lee *et al.* 2012; Berry & Rodeheffer, 2013). During adipocyte development, progenitors first commit to becoming preadipocytes and then further differentiate into adipocytes. Progenitors and pre-adipocytes are the source of adipocytes needed for adipocyte hyperplasia and turnover (Spalding *et al.* 2008). The 'adipose tissue expandability hypothesis' proposes that insufficient availability of precursor to enable increased adipogenesis when challenged with high-energy diet limits adipocyte hyperplasia and hampers replacement of dead adipocytes. Thus, existing adipocytes undergo hypertrophy to accommodate lipids, eliciting hypoxia and inflammation; excessive lipids beyond the storage capacity of adipose tissue accumulate in other tissues, such as skeletal muscle and liver, resulting in insulin resistance and metabolic dysfunction (Tchkonia *et al.* 2010; Virtue & Vidal-Puig, 2010). Thus, maintaining an effective pool of progenitors for adipose expansion and adipocyte replacement is critical for life-course adipose tissue health (Grey & Vidal-Puig, 2007; Zeve *et al.* 2009).

Peroxisome proliferator-activated receptor γ (PPARγ) is a crucial transcription factor that is necessary to induce late stage adipogenesis: the conversion of preadipocytes to adipocytes (Vernochet *et al.* 2009). Recently, zinc finger protein 423 (*zfp423*) was identified as a key regulator of the commitment of progenitors to become preadipocytes. *Zfp423* promotes PPARγ expression and adipogenic differentiation (Gupta *et al.* 2010; Gupta *et al.* 2012). We previously observed that MO reduces DNA methylation in the *zfp423* promoter, which is correlated with enhanced *zfp423* expression and progenitor adipogenesis in fetal mouse tissue (Yang *et al.* 2013). Because DNA methylation is relatively stable, we hypothesized that MO stably elevates *zfp423* expression, thereby predisposing progenitors to premature adipogenic differentiation in offspring adipose tissue. As a result, the adipose tissue of MO offspring has an impaired ability to maintain the progenitor pool. This premature differentiation of offspring progenitor cells limits the corresponding adipose tissue expandability, especially when fed a high-energy diet, leading to adipocyte hypertrophy, a cause of hypoxia and inflammation.

Visceral fat metabolic dysfunction is well correlated with the incidence of diabetes. Therefore, our studies focus on the epididymal fat, a depot that is most commonly used to study the properties of visceral fat in mice (Garin-Shkolnik *et al.* 2014; Yi *et al.* 2014; van Beek *et al.* 2015). Our findings show that MO epigenetically programs offspring adipose tissue progenitors to premature adipogenic differentiation, reducing progenitor density in offspring adipose tissue and their ability to expand when challenged with a high-energy diet.

Methods

Ethical approval

Animal studies were conducted in AAALAC-approved facilities and according to protocols approved by the Institutional Animal Use and Care Committee (IAUCC) of Washington State University. To obtain obese mice, female C57BL/6 mice at 4 weeks of age were fed *ad libitum* either a control diet ($n = 15$) (kcal: 10% energy from fat, 20% from protein and 70% from carbohydrate; D12450H; Research Diets, New Brunswick, NJ, USA) or an obesogenic diet ($n = 18$) (OB; kcal: 45% from fat, 20% from protein and 35% from carbohydrate; D12451; Research Diets) for 8 weeks. Mice were maintained under 12:12 h light/dark cycle with access *ad libitum* to water and food. Females were mated with proven breeder males fed the control diet. During pregnancy and lactation, maternal mice continued to eat their prepregnancy diet. On

Table 1. The primer sequences used for real-time quantitative PCR

Gene	Forward (5′ to 3′)	Reverse (5′ to 3′)	Size (bp)	Accession number
18s	GTAACCCGTTGAACCCCATT	CCATCCAATCGGTAGTAGCG	151	NC_000083.6
aP2	CGACAGGAAGGTGAAGAGCATCATA	CATAAACTCTTGTGGAAGTCACGCCT	158	NM_024406.2
HIF-1α	CGGCGAGAACGAGAAGAAAAAGA	ATCTGTGCCTTCATCTCATCTTCA	249	NM_010431.2
IL-6	GCTGGTGACAACCACGGCCT	AGCCTCCGACTTGTGAAGTGGT	107	NM_031168.1
TNFα	TGGGACAGTGACCTGGACTGT	TTCGGAAAGCCCATTTGAGT	67	NM_001278601.1
MCP1	GCAGTTAACGCCCCACTCA	CCCAGCCTACTCATTGGGATCA	68	NM_011333.3
PPARg2	AGCTCCAAGAATACCAAAGTGCGAT	AGGTTCTTCATGAGGCCTGTTGTAGA	98	XM_006505744.1
PDGFRα	GGACTTACCCTGGAGAAGTGAGAA	ACACCAGTTTGATGGATGGGA	78	XM_006504263.2
Pref1	TGACAATGTCTGCAGGTGCCAT	TATTTCGCAGAATTTCCCGTCC	145	XM_006515457.2
Zfp423	GTCACCAGTGCCCAGGAAGAAGAC	AACATCTGGTTGCACAGTTTACACTCAT	144	XM_006531540.1

postnatal day 1, litters were culled to six pups to ensure the even delivery of maternal nutrition. Mice with litter size less than six pups were excluded from the study. Pups were weaned at postnatal day 21 (P21). Next, two male pups per dam were randomly separated into two subgroups: one pup fed with a regular diet (Reg) and another pup with the same obesogenic diet fed to the maternal OB mice (to avoid confusion, abbreviated as 'Obe') until 3 months of age, which generated four treatment groups: Con/Reg, OB/Reg, Con/Obe and OB/Obe. The food intake and daily energy intake of mice were recorded as described previously (Shankar *et al.* 2008). At the end of treatment, mice were killed by carbon dioxide inhalation and cervical dislocation. Except for special indication, we used epididymal white adipose tissue (EpiWAT) of male offspring for experiments.

Intraperitoneal glucose tolerance test and blood characteristics

The glucose tolerance test was performed as described previously with minor modification (Tong *et al.* 2011). Following 6 h of fasting, 3-month-old offspring were administered 2 g kg^{-1} D-glucose diluted in sterilized water. The blood samples were collected from the tail vein at 0, 15, 30, 60 and 120 min post injection and the glucose concentration was measured by means of the glucose oxidase method using a glucose meter (Bayer Contour, Tarrytown, NY, USA). Blood insulin levels were measured using a Mouse Ultrasensitive Insulin ELISA Kit (catalogue no. 80-INSMSU-E10; ALPCO Diagnostics, Salem, NH, USA) and triglyceride was measured using triglyceride colourimetric assay kit (catalogue no. 10010303; Cayman, Ann Arbor, MI, USA).

Quantitative real-time PCR

Total RNAs were extracted using TRIzol (Life Technologies, Grand Island, NY, USA) and cDNA was synthesized from 500 ng of total RNA using an iScript^{TM} cDNA Synthesis Kit (Bio-Rad, Hercules, CA, USA) in accordance with the manufacturer's instructions. Quantitative real-time PCR was conducted as described previously with 18S rRNA used as a reference (Fu *et al.* 2013). All primers are listed in Table 1.

Immunoblotting analysis

Immunoblotting analyses were carried out as described previously (Yang *et al.* 2013). Polyclonal rabbit antibody against *zfp423* (catalogue no. sc-48785) was purchased from Santa Cruz Biotech (Dallas, TX, USA) and was diluted 1:400. Tubulin antibody (catalogue no. 3873) was purchased from Cell Signalling (Danvers, MA, USA) and was diluted 1:1000. IRDye 800CW goat anti-rabbit (catalogue no. 926-32211) and IRDye 680 goat anti-mouse (catalogue no. 926-68070) secondary antibodies were purchased from LI-COR Biosciences (Lincoln, NE, USA) and were diluted 1:15,000.

Isolation of stromal-vascular cells, cell sorting, *in vitro* differentiation and Oil-Red O staining. Cells in the stromal-vascular fractions (SVFs) of adipose tissue were obtained as described previously (Huang *et al.* 2012). Cell surface markers CD45 (catalogue no. 103114; BioLegend, San Diego, CA, USA) and PDGFRα (catalogue no. 135908; BioLegend) were used to separate progenitor cells from SVFs by flow cytometry. CD45–/PDGFRα+ cells were sorted and harvested. Induction of adipogenic differentiation was conducted as reported previously (Huang *et al.* 2012).

Plasmid transfection. Plasmids pMSCVFLAG-*zfp423* (catalogue no. 24764) and pMKO.1-*zfp423* (catalogue no. 35972) from Addgene (Cambridge, MA, USA) were used for overexpression or knockdown of *zfp423* as described previously (Yang *et al.* 2013).

Bisulphite pyrosequencing. Fetal tissue samples were collected as reported previously (Yang *et al.* 2013). Briefly, fetuses were dissected from the uterus and then the fetal head, heart, lung, liver, surface gelatinous tissue, spinal cord and primordial bones were removed under a dissection microscope. Genomic DNA was isolated from fetal tissue and epididymal adipose tissue using a genomic DNA isolation kit (Qiagen, Redwood City, CA, USA) and 300 ng of genomic DNA was used for bisulphite modification. Bisulphite modification was performed using an EZ DNA methylation-direct kit (catalogue no. D5021; Zymo Research, Irvine, CA, USA). Then, 2 μl of converted genomic DNA was used as the template to amplify the target sequence. The Biotinylated PCR primers were designed to cover 12 CpG sites located between –982 and –908 bp from ATG and –622 to –548 bp from the transcription start site) (Ensembl Transcript ID: ENSMUST00000109655). Hotstar Taq Polymerase (Qiagen) was used for PCR amplification. The PCR cycling conditions were 95 °C for 15 min, followed by 45 × (95 °C for 30 s, 61 °C for 30 s and 72 °C for 30 s), ending with 72 °C for 5 min. Amplicon size was confirmed by electrophoresis. PCR products were sent to EpigenDx (Hopkinton, MA, USA) for pyrosequencing as described previously (Tost & Gut, 2007).

Histochemical staining, adipocyte and progenitor cell quantification. Paraffin-embedded fat tissues were cut to a thickness of 5 μM and subjected to haemotoxylin and eosin (H&E) staining (Yan *et al.* 2010). Adipocye calculations were conducted based on a method described previously (Parlee *et al.* 2014). Images of H&E-stained sections were acquired using an EVOS microscope (Advanced Microscopy Group, Bothell, WA, USA). Four to six images per section and four sections from each individual mouse were acquired. For quantification, the longest and shortest diameters were measured on the images using Image-Pro Plus, version 6.0 (Media Cybernetics, Inc., Rockville, MD, USA) and the average was used for the calculations. Then, adipocyte volume was calculated based on the average adipocyte diameter. The adipocyte number of each fat depot was further calculated by dividing the fat mass by the average adipocyte volume. The expansion ratio of the adipocyte number was calculated by dividing the adipocyte number of the epididymal fat of 3-month-old offspring by that of P21 offspring. The relative pool sizes of PDGFRα positive cells were calculated by multiplying SVF density by the percentage of PDGFRα positive cells obtained via flow cytometry analyses. To obtain the relative SVF density, interstitial 4′,6-diamidino-2-phenylindole positive cells were counted. The relative PDGFRα positive cell density was calculated by dividing the pool size of PDGFRα positive cells by the adipose tissue volume.

Statistical analysis

For cell-related studies, three independent experiments were carried out. For the animal study, each offspring mouse of the same treatment derived from a separate dam was considered as an experimental unit. Data are presented as the mean ± SEM. Data from P21 mice were analysed using an unpaired Student's t test and those from 3-month-old mice were analysed using two-way ANOVA and Tukey's multiple comparison test. $P < 0.05$ was considered statistically significant.

Results

Body composition and adipose tissue characteristics of Con and OB offspring at weaning and 3 months of age

At mating, the body weight of OB dams was heavier than that of Con dams (Con *vs.* OB: 20.9 ± 0.37 *vs.* 27.1 ± 0.71 g; $P < 0.0001$). The concentrations of blood glucose (135 ± 5.3 *vs.* 158 ± 6.4 mg dl^{-1}; $P < 0.05$), insulin (1.2 ± 0.02 *vs.* 1.8 ± 0.11 ng/ml; $P < 0.001$) and triglyceride (85 ± 3.1 *vs.* 98 ± 3.1 mg dl^{-1}; $P < 0.01$) were higher in OB compared to Con dams. The birth weight of OB neonates was higher than that of Con neonates (Con *vs.* OB: 1.2 ± 0.01 *vs.* 1.3 ± 0.02 g; $P < 0.01$).

At weaning (P21), OB offspring were heavier than Con offspring ($P < 0.0001$) (Fig. 1*A*). The EpiWAT of OB offspring (Con *vs.* OB; 35 ± 3.1 *vs.* 91 ± 3.3 mg; $P < 0.0001$) was much larger compared to Con offspring, as also was the case for inguinal white adipose tissue (IngWAT) (Con *vs.* OB; 90 ± 4.0 *vs.* 157 ± 4.9 mg; $P < 0.0001$). The difference in mass of EpiWAT and IngWAT was maintained after normalization for body weight ($P < 0.0001$) (Fig. 1*B*). When stained with H&E, OB adipose tissue had more abundant adipocytes with larger diameters (Fig. 1*C*). In brief, MO increased offspring fat mass, especially for the visceral fat at weaning.

At 3 months of age, regardless of maternal treatment, the body weight of offspring on the high-energy diet was greater than that of offsprong on a regular diet, which is consistent with their levels of energy intake (Fig. 1*D* and *E*). MO had no effect on offspring body weight when fed a regular diet, although OB/Obe mice were heavier than Con/Obe mice with no difference in energy intake (Fig. 1*D* and *E*). There was no difference in EpiWAT and IngWAT mass between Con/Reg and OB/Reg mice, although fat mass was greater in OB/Obe than Con/Obe mice (Fig. 1*F* and *G*). Large adipocytes were most abundant in OB/Obe mice, followed by Con/Obe mice, with no difference between Con/Reg and OB/Reg mice (Fig. 1*H* and *I*), which is consistent with the differences in average adipocyte diameters (Fig. 1*J*). Newly-formed adipocytes have smaller sizes; note that the OB/Obe tissue section was largely

absent of small adipocytes, indicating a lower rate of *de novo* adipogenesis in the EpiWAT of OB/Obe mice.

Adipocyte number in adipose tissue of Con and OB offspring at weaning and 3 months of age

At weaning, the number of adipocytes in EpiWAT was greater in the offspring of obese mothers (Fig. 2*A*). At 3 months of age, the number of adipocytes was increased in EpiWAT, although there was no difference among all treatments (Fig. 2*B*). The number of adipocytes in EpiWAT increased by 157.2 ± 11.52% for Con/Reg and 281.3 ± 5.27% for Con/Obe offspring compared to the offspring of obese mothers where the number of adipocytes increased by 91.8 ± 47.03% for OB/Reg and 141.1 ± 22.02% for OB/Obe mice (Fig. 2*A* and *B*). Consistently, Con/OB mice had the highest adipocyte expansion ratio, whereas that for OB/Obe was much lower than Con/Obe mice ($P < 0.01$) (Fig. 2*C*). Similar changes were observed in IngWAT at weaning (Fig. 2*D*), as well as at 3 months (increase of 404.2 ± 38.31% for Con/Reg and 500.4 ± 54.23% for Con/Obe) and for the offspring of obese mothers (increase of 295.8 ± 28.47% for OB/Reg and 263.1 ± 80.24% for OB/Obe) (Fig. 2*E* and

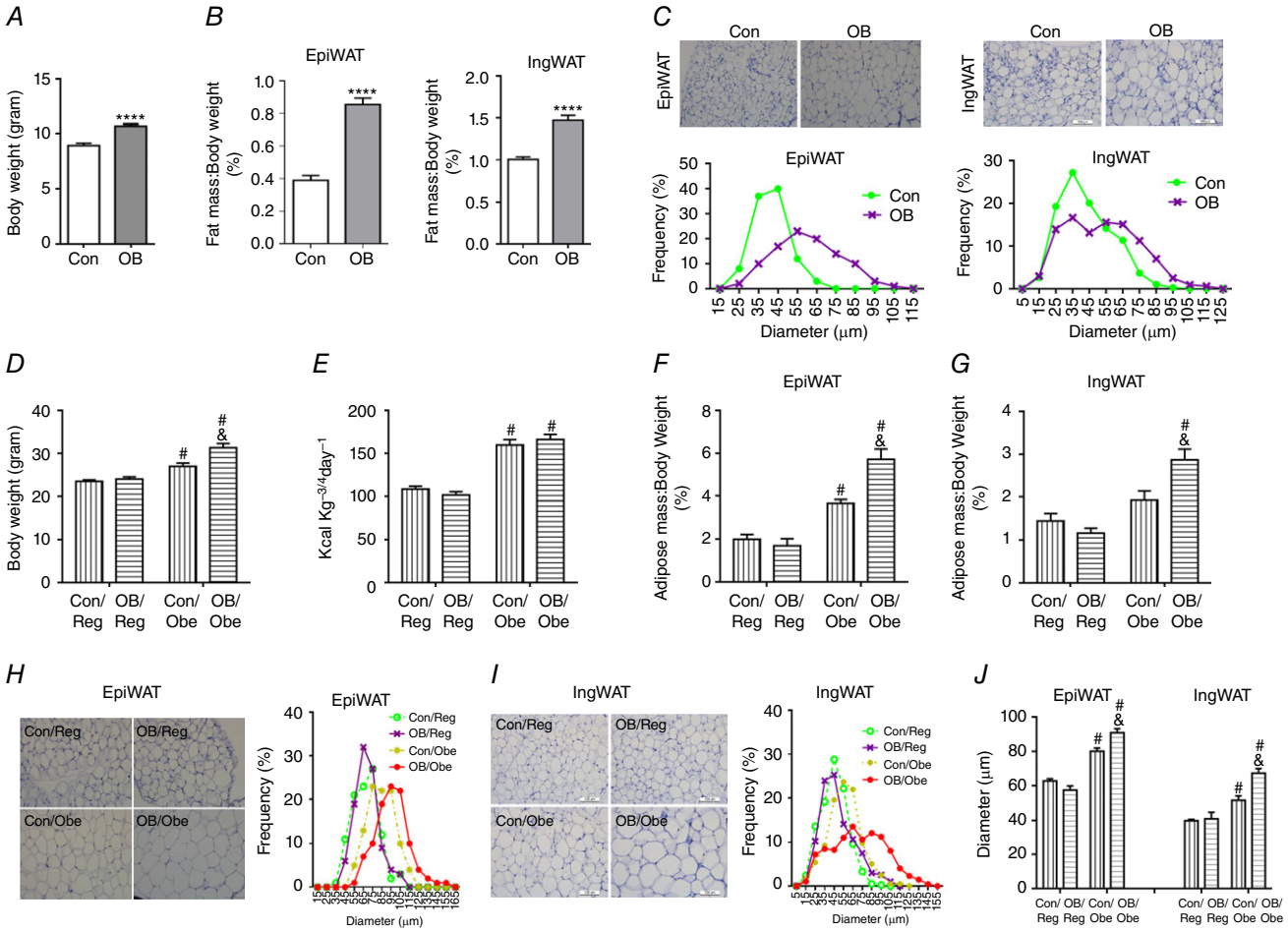

Figure 1. Body weight and adipose tissue characteristics of offspring of Con and OB dams at weaning (*A–C*) and at 3 months of age (*D–J*)
A, body weight of offspring of Con and OB dams at weaning (P21) (Con: $n = 13$; OB: $n = 7$). *B*, fat index (percentage of fat weight normalized to the body weight) of EpiWAT and IngWAT of offspring at P21 (Con: $n = 13$; OB: $n = 7$). *C*, representative images of H&E staining and adipocyte distribution of EpiWAT and IngWAT at P21. *D* and *E*, body weight (*D*) and caloric intake (*E*) of Con and OB offspring weaned on regular or obesogenic diets ($n = 6$). *F* and *G*, fat index of EpiWAT (*F*) and IngWAT (*G*) of 3-month-old offspring ($n = 6$). *H* and *I*, representative images of H&E staining and adipocyte distribution of EpiWAT (*H*) and IngWAT (*I*) of offspring at 3 months of age. *J*, average diameters of adipocytes in EpiWAT and IngWAT of offspring at 3 months of age. Data are expressed as the mean ± SEM. For offspring at weaning: $^{****}P < 0.0001$ *vs.* Con as determined using Student's *t* test. For 3-month-old offspring: $^{\&}P < 0.05$ *vs.* Con within the same post-weaning diet and $^{\#}P < 0.05$ *vs.* post-weaning Reg within the same maternal diet as determined by two-way ANOVA and Tukey's multiple comparison.

F). Con/Obe mice had a trend for an increase compared to OB/Obe mice ($P = 0.10$) (Fig. 2*F*). These data demonstrate that adipocyte hyperplasia under excessive energy intake was hampered in the EpiWAT of the offspring of obese mothers, which partially explained the hypertrophy of adipocytes in OB/Obe offspring (Fig. 1*H–J*).

Density of progenitor cells in the epididymal fat at weaning and 3 months of age

At weaning, we sorted putative adipogenic progenitor cells in SVFs prepared from EpiWAT with cell surface markers, CD45 and PDGFRα, and did not observe any difference in the ratio of CD45–/PDGFRα+ cells between Con and OB offspring (Fig. 3*A*). Constantly, the total number of progenitors in EpiWAT did not differ at weaning (Fig. 3*B*). On the other hand, the density was lower in the OB group (Fig. 3*C*). In agreement, there was no difference in mRNA expression of PDGFRα, nor the expression of preadipocyte factor 1 (Pref-1), a marker of preadipocytes (Fig. 3*D*).

At 3 months of age, the ratio of CD45–/PDGFRα+ cells was dramatically lower in OB/Obe mice (~50% less than OB/Reg and Con/Obe; $P < 0.05$) (Fig. 3*E* and *F*). Because adipose tissue expansion requires the extensive proliferation and adipogenic differentiation of progenitor cells, the reduction in the ratio of CD45–/PDGFRα+ cells in OB/Obe mice was consistent with the reduction in adipose expansion capacity in these mice (Fig. 2). On the other hand, the ratio of CD45–/PDGFRα+ cells in Con/Obe mice was higher than in Con/Reg mice, indicating the expansion of progenitors ($P < 0.05$) (Fig. 3*E* and *F*). We further calculated the total number of progenitors (pool size) in EpiWAT. Although there was only a trend for a difference between OB/Obe and Con/Obe mice ($P = 0.08$) (Fig. 3*G*), the density of progenitors was lower in OB/Obe mice ($P < 0.05$) (Fig. 3*H*). In brief, the reduction in progenitor density in OB/Obe compared to Con/Obe mice highlights the programming effects of MO on the progenitor properties of offspring under the high-energy diet environment.

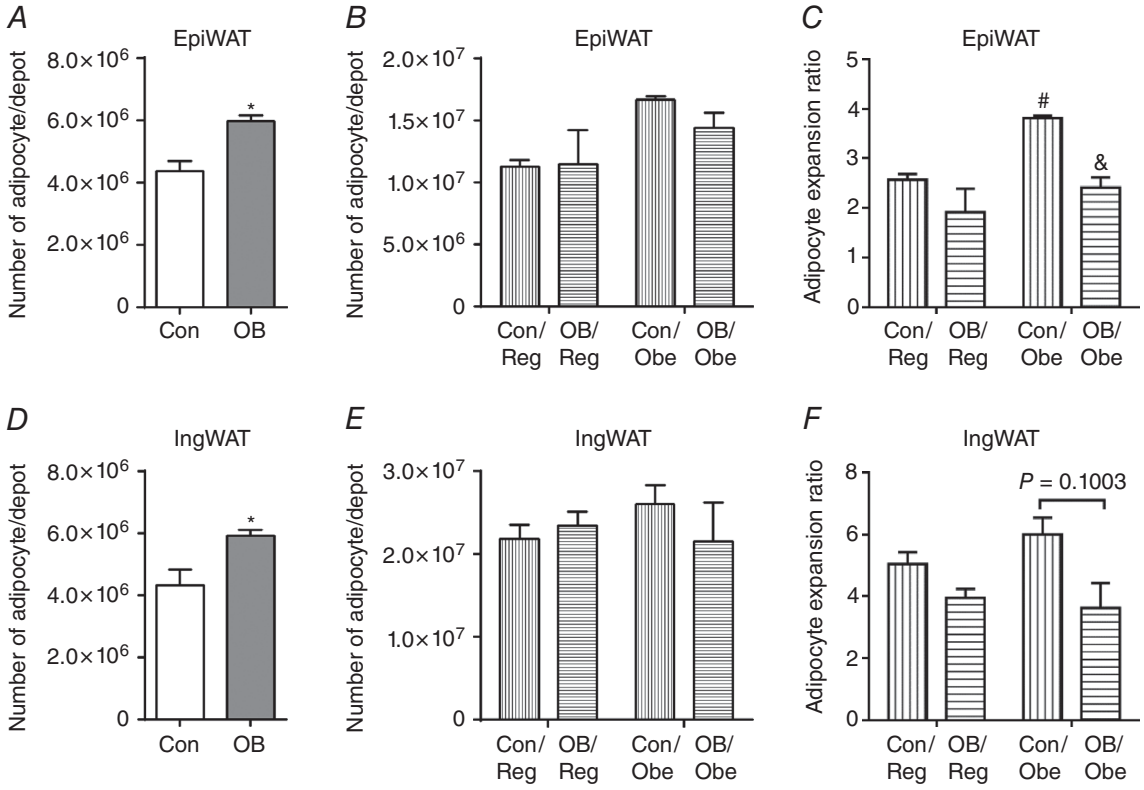

Figure 2. Adipocyte pool in fat depots of weaning (P21) (*A* and *D*) and 3-month-old (*B, C, E* and *F*) offspring
A and *B*, the number of adipocytes in EpiWAT at P21 (*A*) and at 3 months of age (*B*); *C*, adipocyte expansion in EpiWAT of 3-month-old offspring relative to P21 from the dams fed the same diet. *D* and *E*, number of adipocytes in IngWAT at P21 (*D*) and at 3 months of age (*E*). *F*, adipocyte expansion in IngWAT of 3-month-old offspring relative to P21 from the dams fed with the same diet. Data are expressed as the mean ± SEM ($n = 6$). For offspring at P21, $^{*}P < 0.05$ *vs*. Con as determined using Student's *t* test. For 3-month-old offspring: $^{\&}P < 0.05$ *vs*. Con within the same post-weaning diet as determined by two-way ANOVA and Tukey's multiple comparison.

zfp423 DNA methylation and adipogenic differentiation of progenitor cells from the epididymal fat of Con and OB offspring at weaning

First, we tested the role of *zfp423* in the adipogenic differentiation of progenitor cells. We separated progenitor cells (CD45–/PDGFRα+) from wild-type mice at weaning, and transfected with plasmids to either overexpression or knockdown of *zfp423*. *zfp423* overexpression enhanced and knockdown inhibited the adipogenic differentiation, as indicated by the expression of adipogenic markers, PPARγ and adipocyte protein 2 (aP2) (Fig. 4*A* and *B*), confirming the critical role of *zfp423* in regulating adipogenic differentiation in progenitor cells.

At weaning, *zfp423* mRNA expression was ∼3-fold higher in OB compared to Con offspring EpiWAT (Fig. 5*A*). Consistently, the protein content of *zfp423* was also much higher in OB offspring (Fig. 5*B*). We further analysed DNA methylation in the shore area of the CpG island of the *zfp423* promoter, which we previously identified to have differential methylation between control and OB fetal samples (Yang *et al.* 2013). Using pyrosequencing, we found that the DNA methylation in eight out of 12 CpG sites analysed was lower in OB compared to Con samples; the overall methylation was reduced (Con *vs.* OB; 5.5 ± 0.14% *vs.* 3.1 ± 0.15%; $P < 0.01$) (Fig. 5*C*). In combination, these data clearly show that MO enhanced *zfp423* expression in the EpiWAT at weaning, which is associated with lower DNA methylation in the *zfp423* promoter.

To analyse specific changes in progenitor cells, we separated CD45–/PDGFRα+ progenitor cells and analysed *zfp423* mRNA expression and DNA methylation in the promoter. Consistently, OB progenitor cells had

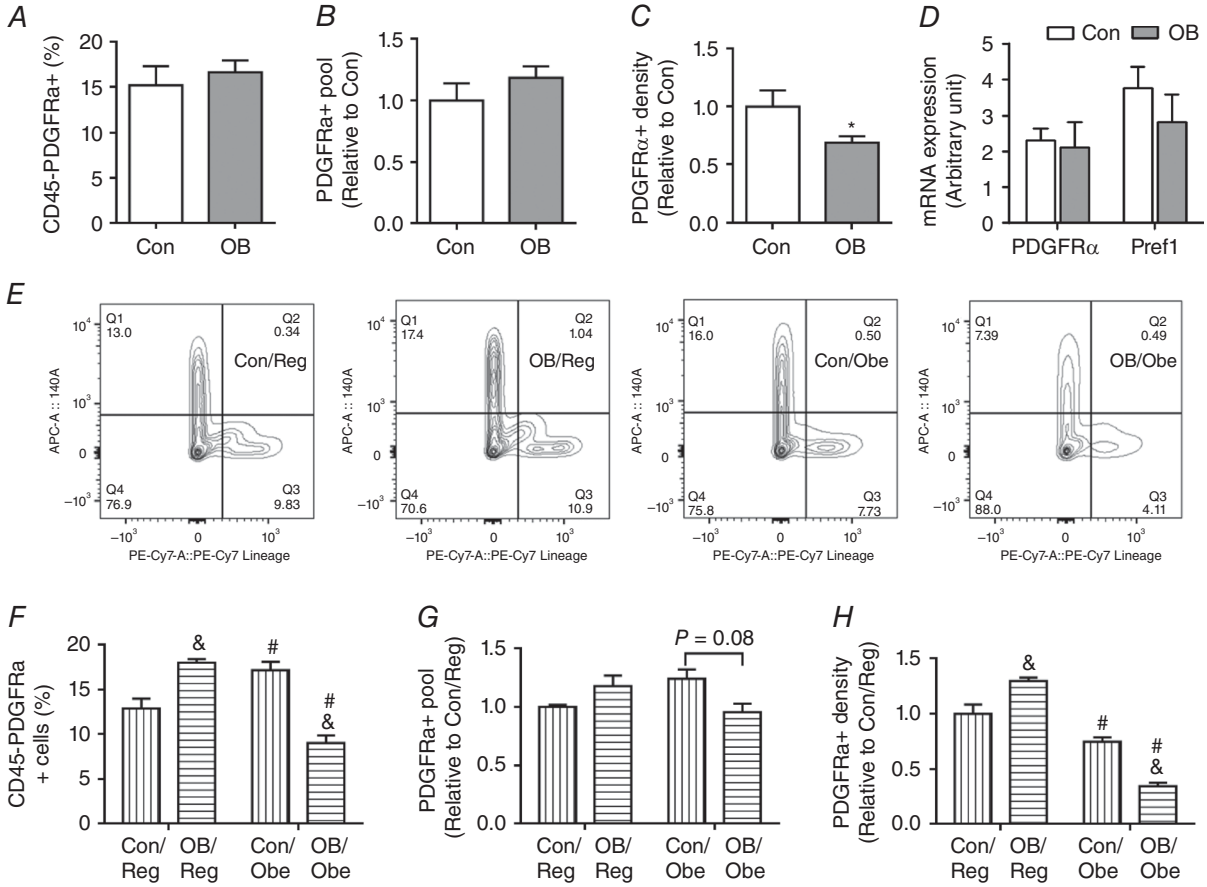

Figure 3. Progenitor cells in epididymal fat (EpiWAT) of Con and OB offspring
A, percentage of CD45–/PDGFRα+ cells of stromal vascular cells at P21. *B*, the pool size of progenitors in EpiWAT at P21. *C*, the density of progenitors at P21. *D*, mRNA expression of PDGFRα and Pref1 in EpiWAT at P21. *E*, representative flow cytometry data sorted by using CD45– and PDGFRα+ at 3 months of age. *F*, percentage of CD45–/PDGFRα+ cells at 3 months of age. *G*, the pool sizes of progenitors at 3 months of age. *H*, density of progenitors at 3 months of age. Data are expressed as the mean ± SEM ($n = 6$). For offspring at weaning: $^{*}P < 0.05$ *vs.* Con as determined using Student's *t* test. For 3-month-old offspring: $^{\&}P < 0.05$ *vs.* Con within the same post-weaning diet and $^{\#}P < 0.05$ *vs.* post-weaning Reg within the same maternal diet as determined by two-way ANOVA and Tukey's multiple comparison.

much higher *zfp423* mRNA expression compared to Con (Fig. 5*D*), which is associated with reduced *zfp423* DNA methylation (Fig. 5*E*). The adipogenic differentiation was higher in OB compared to Con progenitor cells (Fig. 5*F*). Correspondingly, mRNA expression of adipogenic marker genes, PPARγ and aP2, was also higher in OB cells (Fig. 5*G*). Taken together, these data show that MO enhances the adipogenic differentiation of progenitor cells at weaning.

zfp423 DNA methylation and adipogenic differentiation of progenitor cells from the epididymal fat of Con and OB offspring at 3 months of age

To assess its long-term impact, we analysed mRNA expression and the protein content of *zfp423* in adipose tissue of 3-month-old offspring mice. Although there were no significant differences in *zfp423* mRNA expression in EpiWAT, the overall trend appeared to be OB/Obe > Con/Obe > OB/Reg > Con/Reg (OB/Obe *vs.* Con/Reg; $P = 0.06$) (Fig. 6*A*). OB/Obe mice had higher *zfp423* protein contents compared to OB/Reg ($P < 0.05$) or Con/Obe ($P < 0.05$) mice (Fig. 6*B*). In progenitor cells, OB/Obe mice had the highest *zfp423* expression (Fig. 6*C*). In keeping with these findings, progenitor cells of OB/Obe mice demonstrated the highest adipogenic differentiation capacity indicated both by Oil-Red O staining (Fig. 6*D*) and by mRNA expression of adipogenic markers, PPARγ and aP2 (Fig. 6*E*). We then analysed DNA methylation by pyrosequencing. Indeed, the EpiWAT (Fig. 6*F*) and progenitor cells (Fig. 6*G*) of OB/Obe mice had lower DNA methylation in the *zfp423* promoter compared to other treatments. Of note, the level of DNA methylation was less than 2% for all samples, which was much lower than the DNA methylation in the progenitors at weaning, where the DNA methylation levels were 7.3 ± 2.37% (Fig. 5*E*). Consistently, the reduction of DNA methylation in the *zfp423* promoter also took place during adipose tissue development. It was very low at embryonic day 13.5 (E13.5, 2.7 ± 0.76%; E13.5 *vs.* P21; $P < 0.01$), then peaked E17.5 (7.7 ± 1.01%) and was followed by a reduction to 2.9 ± 0.11% at 3 months of age (3 months *vs.* P21; $P < 0.0001$), in line with data obtained from progenitor cells and adipose tissue of 3-month-old offspring (Fig. 6*F* and *G*).

Inflammation and hypoxic response in adipose tissue and glucose tolerance test in 3-month-old offspring

The expression of both interleukin (IL)-6 and tumor necrosis factor (TNF)α was increased when the offspring were subjected to a high-energy diet compared to the regular diet, whereas there was no maternal effect under the same post-weaning diet (Fig. 7*A* and *B*). The expression of macrophage chemotactic protein (MCP)-1, an important cytokine attracting macrophage infiltration (McCurdy *et al.* 2012), was highest in OB/Obe mice (Fig. 7*C*), as also was the case for the expression of hypoxia-inducible factor 1α (Fig. 7*D*). Compared to OB/Obe mice, expression levels were lower in Con/Obe mice, showing that MO had programming effects on adipose metabolic dysfunction. These data are in line with the enhanced adipocyte sizes in the EpiWAT of OB/Obe mice. In combination, our data strongly support the notion that a reduced expansion capacity leads to unhealthy adipose tissue when challenged with a high-energy diet.

Consistently, following the glucose challenge, the rate of glucose clearance was similar in OB/Reg and Con/Reg

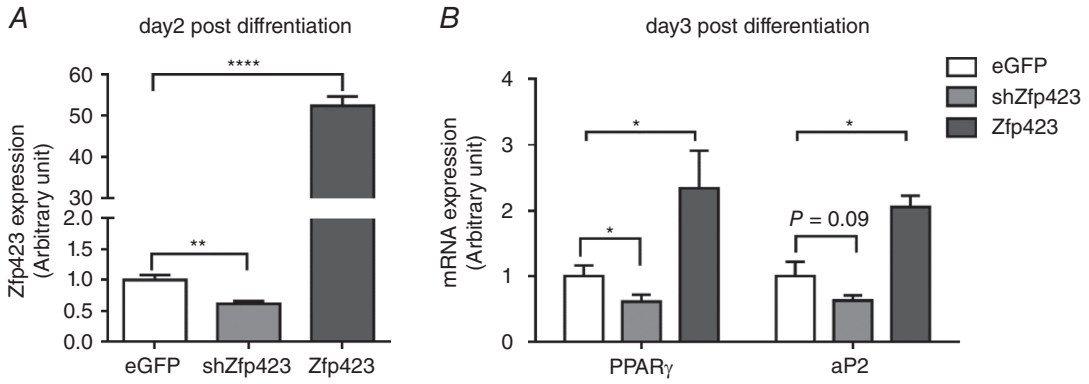

Figure 4. *zfp423* regulated adipogenesis of progenitor cells derived from adipose tissue
Progenitors were separated from adipose tissue of wild-type mice at weaning and transfected with enhanced green fluorescent protein control vector, *zfp423* overexpression vector or *zfp423* shRNA vector, and then adipogenic differentiation was induced. *A*, mRNA expression of *zfp423* at 2 days of adipogenic differentiation. *B*, mRNA expression of PPARγ and aP2 at 3 days of adipogenic differentiation. Data were analysed by a *t* test *vs.* control ($n = 3$; $^*P < 0.05$; $^{**}P < 0.01$; $^{****}P < 0.0001$; data are the mean ± SEM).

mice, although it was reduced in OB/Obe compared to Con/Obe mice (Fig. 7*E* and *F*). We further measured the blood insulin and found that there was no difference between Con/Reg and OB/Reg mice, although OB/Obe mice had a higher blood insulin level compared to Con/Obe mice (Fig. 7*G*). A similar change was also observed with respect to the blood triglyceride level (Fig. 7*H*). All these data indicate that MO programs the metabolic dysfunction in offspring that are challenged with a high-energy diet.

Discussion

Recent studies suggest that insufficient adipogenesis in response to excessive dietary energy intake is a critical mechanism leading to adipose tissue inflammation and metabolic dysfunction: the 'adipose tissue expandability hypothesis' (Tchkonia *et al.* 2010; Virtue & Vidal-Puig, 2010). In this situation, as a result of the limited capacity to generate new adipocytes, existing adipocytes undergo hypertrophy to accommodate excessive fatty acids, and overflow fatty acids spill over to other tissues, incurring ectopic lipid deposition, insulin resistance and dyslipidaemia (Sun *et al.* 2011; Michaud *et al.* 2012). Consistent with this notion, lipodystrophy, a condition with decreased adipose tissue, leads to severe insulin resistance and dyslipidaemia (Huang-Doran *et al.* 2010), whereas enhancing adipogenesis increases fat mass and improves insulin sensitivity (Okuno *et al.* 1998; de Souza *et al.* 2001). The impact of adipose expandability on metabolic dysfunction is greater in the visceral fat because it has a lower capacity for expansion than the subcutaneous fat (Greenwood & Hirsch, 1974; Bertrand *et al.* 1978; van Beek *et al.* 2015). Visceral fat mass and adipocyte

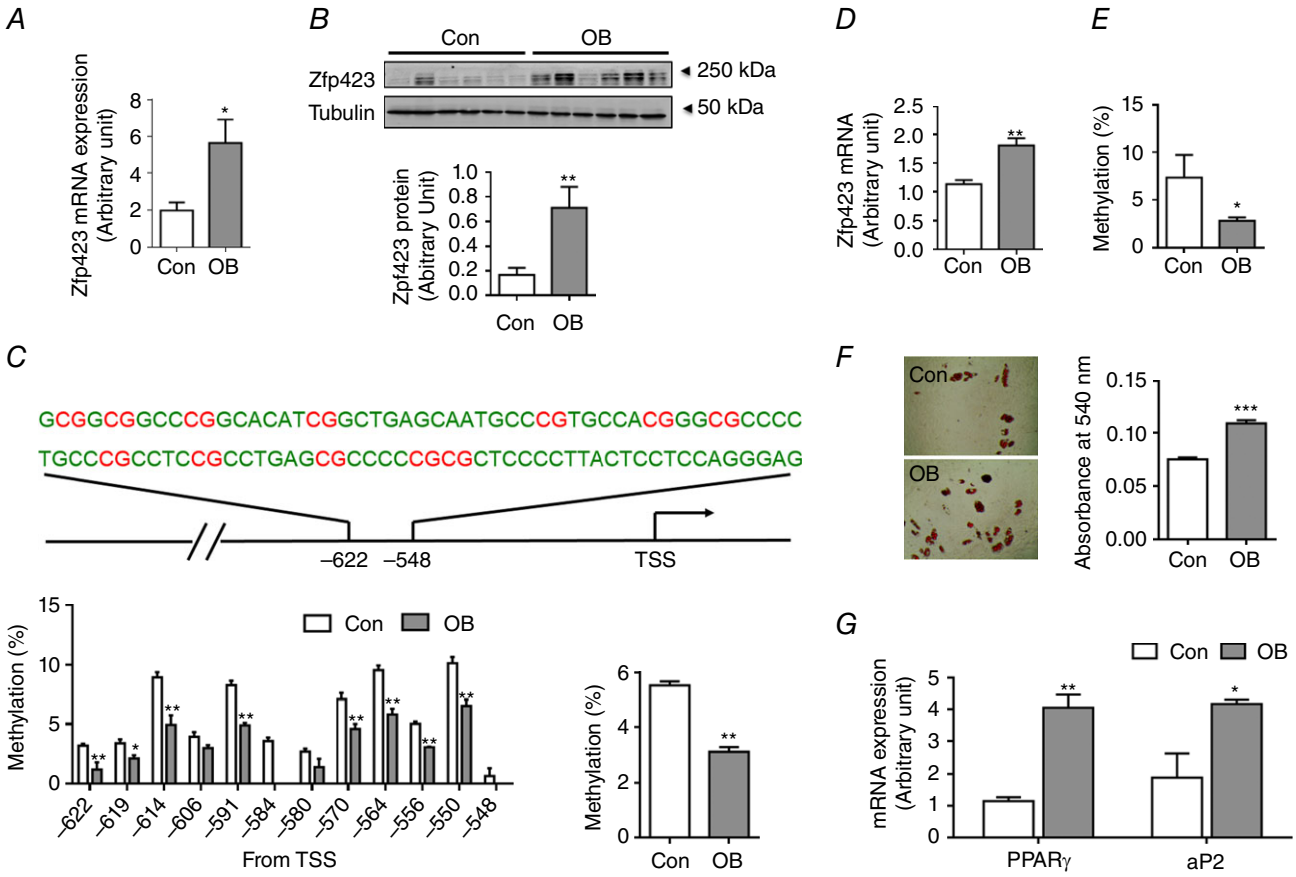

Figure 5. *zfp423* expression, DNA methylation of the *zfp423* promoter, and differentiation of progenitors of adipose tissue and progenitor cells at weaning
PDGFRα+/CD45– progenitors were separated by flow cytometry. *A* and *B*, *zfp423* mRNA expression (*A*) and protein content (*B*) in EpiWAT ($n = 6$). *C*, DNA methylation in the *zfp423* promoter of EpiWAT (12 CpG sites, highlighted in red, was measured in the *zfp423* promotor, and the percentage of methylation of each site is shown, as well as the average DNA methylation) ($n = 6$). *D*, *Zfp423* mRNA expression in progenitor cells. *E*, DNA methylation in the *zfp423* promoter of progenitor cells ($n = 6$). *F*, Oil-Red O staining of the presence of adipocytes and quantification of fat content after 8 days of adipogenic differentiation ($n = 3$). *G*, mRNA expression of adipogenic markers, PPARγ and aP2, after 8 days of adipogenic differentiation ($n = 3$). Data are expressed as the mean ± SEM. $^{*}P < 0.05$; $^{**}P < 0.01$; $^{***}P < 0.001$ *vs.* Con as determined using Student's *t* test.

size are well correlated with diabetes, hyperlipidaemia and cardiovascular diseases (Einstein *et al.* 2008; Ross *et al.* 2008; Klein, 2010). Epididymal fat is the most commonly used fat for studying visceral fat properties in mice (Garin-Shkolnik *et al.* 2014; Yi *et al.* 2014; van Beek *et al.* 2015) and MO programs obesity and increases epididymal fat mass in offspring (Samuelsson *et al.* 2008; Tong *et al.* 2011). Given the sex dimorphism and depot difference in fat tissue function (Lemieux *et al.* 1993; White & Tchoukalova, 2014), the present study focused on the epididymal fat of male offspring aiming to explore the mechanistic impact of MO on offspring obesity and metabolic disorders. We expect that similar mechanisms should also be applicable to females considering the conservativeness of adipogenic mechanisms.

Approximately 10% of fat cells are renewed annually at all adult ages (Spalding *et al.* 2008). The renewal of adipocytes requires the *do novo* differentiation of pre-adipocytes that derive from the commitment of adipocyte progenitors (Gupta *et al.* 2012; Berry & Rodeheffer, 2013). PDGFRα positive cells residing in adipose tissue are the source of white adipocytes (Lee *et al.* 2012; Berry & Rodeheffer, 2013). In our previous study, we found that MO enhanced the adipogenesis of fetal progenitors (Yang *et al.* 2013). Because the offspring adipogenic progenitor cells are derived from fetal progenitor cells, in the present study, we further explored the long-term changes in progenitor properties of offspring EpiWAT. We used PDGFRα as a marker to identify adipocyte progenitors and found that the progenitor density in OB/Obe mice

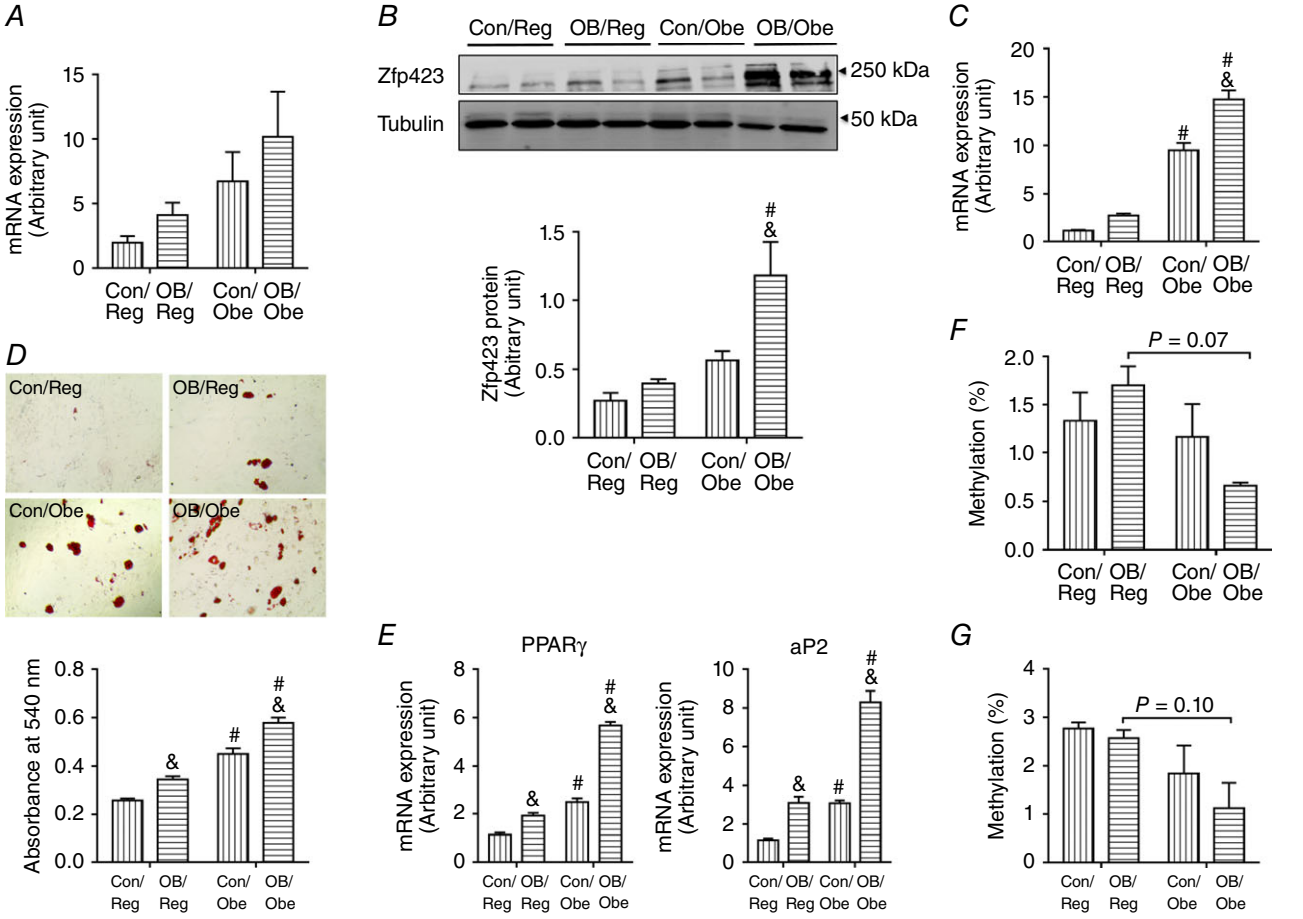

Figure 6. *zfp423* expression, DNA methylation of the *zfp423* promoter, and differentiation of progenitors of adipose tissue and progenitor cells at 3-month-old offspring
A and *B*, *zfp423* mRNA expression (*A*) and protein content (*B*) in EpiWAT of 3-month-old offspring ($n = 6$). *C*, *zfp423* mRNA expression in CD45–/PDGFRα+ progenitor cells ($n = 6$). *D*, Oil-Red O staining of CD45–/PDGFRα+ progenitor cells and quantification of fat content after 8 days of adipogenic differentiation ($n = 3$). *E*, mRNA expression of adipogenic markers, PPARγ and aP2, after 8 days of adipogenic differentiation ($n = 3$). *F*, the average methylation level of the *zfp423* promoter in adipose tissue assayed by bisulphite pyrosequencing ($n = 6$). *G*, the average methylation level of the *zfp423* promoter in progenitor cells assayed by bisulphite pyrosequencing ($n = 6$). Data are expressed as the mean ± SEM. $^{\&}P < 0.05$ *vs.* Con within the same post-weaning diet and $^{\#}P < 0.05$ *vs.* post-weaning Reg within the same maternal diet as determined by two-way ANOVA and Tukey's multiple comparison.

was lower than Con/Obe mice, which is consistent with our hypothesis that the premature adipogenic differentiation of OB progenitor cells leads to their exhaustion in adipose tissue. In addition, when compared with adipose tissue at weaning, the ratio of expansion was much smaller in OB/Obe mice compared to Con/Obe mice, clearly showing the limited adipose expansion in OB offspring when challenged with a high-energy diet. Of note, in the present study, two-dimensional quantification of adipocyte sizes of sectioned tissue samples was employed. Because this method could not distinguish between whether the shortest diameter represents the midline section of a small adipocyte or the off-midline sectioning of a larger adipocytes, the average adipocyte sizes measured would be smaller than the actual adipocyte sizes. Fortunately, because the same method was used for adipocyte measurement of all samples, the chances of off-midline sectioning were almost equivalent and would not affect the ratio of adipocyte expansion among treatments, which we were comparing in the present study.

zfp423 is the key regulator that determines the fate of adipocyte progenitors to preadipocytes, and it further promotes adipogenic differentiation by inducing PPARγ expression (Gupta *et al.* 2010; Gupta *et al.* 2012). We have previously reported that MO promoted the adipogenesis of fetal progenitor cells, which was associated with the enhanced expression of *zfp423* and reduced DNA methylation of its promoter (Yang *et al.* 2013). These observations prompted us to further examine whether such an epigenetic change is maintained in progenitor cells in offspring adipose tissue. Consistently, at weaning, DNA methylation in the *zfp423* promoter remained lower in OB cells compared to Con cells, which was correlated with enhanced *zfp423* expression and elevated adipogenic differentiation of progenitor cells. Our data are supported by the results of another study in rats showing enhanced *zfp423* expression in adipose tissue of OB offspring (Borengasser *et al.* 2013).

We also analysed *zfp423* DNA methylation both in adipose tissue and in progenitor cells at 3 months of age. Intriguingly, we found that the DNA methylation level of the *zfp423* promoter in adipose tissue of all treatments was dramatically lower than that at weaning, showing that a demethylation process probably occurred during adipose development, which has not been reported previously. To confirm this novel observation, we analysed the DNA methylation of the *zfp423* promoter during adipose tissue development. We found that the methylation level peaked around E17.5 and demethylation occurred during further development. We also found that the DNA methylation

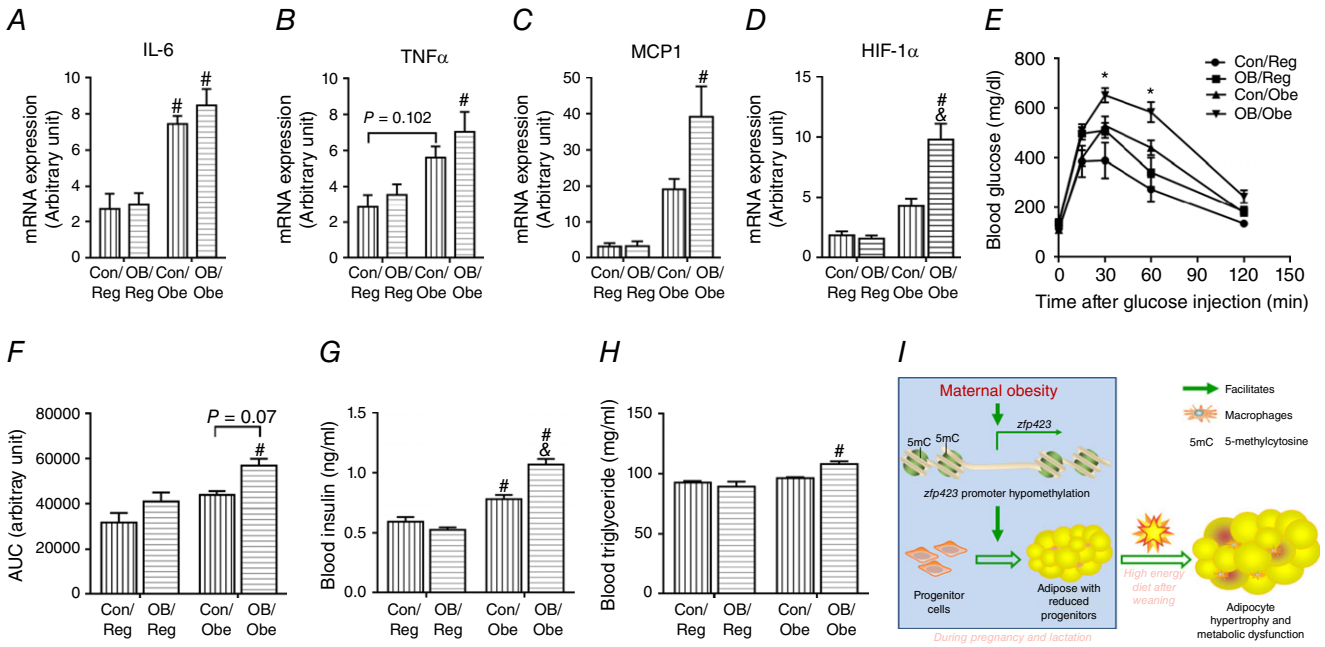

Figure 7. Whole body glucose tolerance, inflammation and hypoxia in the epididymal fat (EpiWAT) of 3-month-old offspring
A–D, mRNA expression of IL-6 (*A*), TNFα (*B*), MCP-1 (*C*) and HIF-1α (*D*) in EpiWAT ($n = 6$). *E*, total body glucose tolerance test. *F*, areas under the curves to measure glucose clearance ability ($n = 4$). *G–H*, blood insulin (*G*) and triglyceride (*H*) levels ($n = 6$). *I*, the underlying mechanism linking maternal obesity to adipose metabolic dysfunction in offspring. Data are expressed as the mean ± SEM. $^{*}P < 0.05$ *vs.* all other groups determined by repeated-measures ANOVA. $^{\&}P < 0.05$ relative to Con within the same post-weaning diet and $^{\#}P < 0.05$ relative to post-weaning Reg within the same maternal diet as determined by two-way ANOVA and Tukey's multiple comparison.

was lower in OB compared to Con mice at weaning, which was correlated with lower DNA methylation both in progenitors and in adipose tissue of OB/Obe compared to Con/Obe mice. In short, these data suggest that DNA demethylation occurred in the *zfp423* promoter during adipose development, which was accelerated in the progenitor cells and adipose tissue of OB offspring challenged with a high-energy diet.

Aligned with lower expansion capacity, OB/Obe adipose tissue had larger adipocytes, which were associated with hypoxic and inflammatory responses, both of which are known to induce adipose tissue metabolic dysfunction (Gustafson *et al.* 2009; Lee *et al.* 2014). Furthermore, global glucose clearance ability was also impaired in OB/Obe mice. Our finding is supported by previous studies reporting that impairment of adipocyte turnover is associated with insulin resistance (Kim *et al.* 2014). Of note, the offspring mice in the present study were only 3 months old, and the detection of hypoxia and inflammation in adipose tissue at such a young age accentuates the significance of these adverse effects of MO on the adipose function of offspring, which probably worsens with advancing age (Kim *et al.* 2014).

In summary, MO induces persistent epigenetic changes in the key developmental gene regulating adipogenesis in the offspring adipose tissue, thereby impairing the renewal of progenitor cells during adipose expansion, which sequentially impairs the ability of adipose tissue to undergo further expansion, resulting in adipocyte hypertrophy, a cause of hypoxia and inflammation (Fig. 6*G*). These insights identify a key novel mechanism linking MO to obesity and metabolic dysfunction in offspring, and open a new window for studying 'developmental programming' by focusing on epigenetic changes in adipocyte progenitors.

References

Berry R & Rodeheffer MS (2013). Characterization of the adipocyte cellular lineage in vivo. *Nat Cell Biol* **15**, 302–308.

Bertrand HA, Masoro EJ & Yu BP (1978). Increasing adipocyte number as the basis for perirenal depot growth in adult rats. *Science* **201**, 1234–1235.

Biro FM & Wien M (2010). Childhood obesity and adult morbidities. *Am J Clin Nutrit* **91**, 1499S–1505S.

Blackmore HL, Niu Y, Fernandez-Twinn DS, Tarry-Adkins JL, Giussani DA & Ozanne SE (2014). Maternal diet-induced obesity programs cardiovascular dysfunction in adult male mouse offspring independent of current body weight. *Endocrinology* **155**, 3970–3980.

Borengasser SJ, Zhong Y, Kang P, Lindsey F, Ronis MJ, Badger TM, Gomez-Acevedo H & Shankar K (2013). Maternal obesity enhances white adipose tissue differentiation and alters genome-scale DNA methylation in male rat offspring. *Endocrinology* **154**, 4113–4125.

de Souza CJ, Eckhardt M, Gagen K, Dong M, Chen W, Laurent D & Burkey BF (2001). Effects of pioglitazone on adipose tissue remodelling within the setting of obesity and insulin resistance. *Diabetes* **50**, 1863–1871.

Desai M, Jellyman JK & Ross MG (2015). Epigenomics, gestational programming and risk of metabolic syndrome. *Int J Obes (Lond)* **39**, 633–641.

Einstein FH, Fishman S, Muzumdar RH, Yang XM, Atzmon G & Barzilai N (2008). Accretion of visceral fat and hepatic insulin resistance in pregnant rats. *Am J Physiol Endocrinol Metab* **294**, E451–E455.

Flegal KM, Carroll MD, Kit BK & Ogden CL (2012). Prevalence of obesity and trends in the distribution of body mass index among US adults, 1999–2010. *JAMA* **307**, 491–497.

Fu X, Zhao JX, Zhu MJ, Foretz M, Viollet B, Dodson MV & Du M (2013). AMP-activated protein kinase alpha1 but not alpha2 catalytic subunit potentiates myogenin expression and myogenesis. *Mol Cell Biol* **33**, 4517–4525.

Garin-Shkolnik T, Rudich A, Hotamisligil GS & Rubinstein M (2014). FABP4 attenuates PPARgamma and adipogenesis and is inversely correlated with PPARgamma in adipose tissues. *Diabetes* **63**, 900–911.

Grey SL & Vidal-Puig AJ (2007). Adipose tissue expandability in the maintenance of metabolic homeostasis. *Nutr Rev* **65**, S7–S12.

Greenwood MR & Hirsch J (1974). Postnatal development of adipocyte cellularity in the normal rat. *J Lipid Res* **15**, 474–483.

Gupta RK, Arany Z, Seale P, Mepani RJ, Ye L, Conroe HM, Roby YA, Kulaga H, Reed RR & Spiegelman BM (2010). Transcriptional control of preadipocyte determination by Zfp423. *Nature* **464**, 619–623.

Gupta RK, Mepani RJ, Kleiner S, Lo JC, Khandekar MJ, Cohen P, Frontini A, Bhowmick DC, Ye L, Cinti S & Spiegelman BM (2012). Zfp423 expression identifies committed preadipocytes and localizes to adipose endothelial and perivascular cells. *Cell Metab* **15**, 230–239.

Gustafson B, Gogg S, Hedjazifar S, Jenndahl L, Hammarstedt A & Smith U (2009). Inflammation and impaired adipogenesis in hypertrophic obesity in man. *Am J Physiol Endocrinol Metab* **297**, E999–E1003.

Huang-Doran I, Sleigh A, Rochford JJ, O'Rahilly S & Savage DB (2010). Lipodystrophy: metabolic insights from a rare disorder. *J Endocrinol* **207**, 245–255.

Huang Y, Das AK, Yang QY, Zhu MJ & Du M (2012). Zfp423 promotes adipogenic differentiation of bovine stromal vascular cells. *PloS ONE* **7**, e47496.

Kim SM, Lun M, Wang M, Senyo SE, Guillermier C, Patwari P & Steinhauser ML (2014). Loss of white adipose hyperplastic potential is associated with enhanced susceptibility to insulin resistance. *Cell Metab* **20**, 1049–1058.

Klein S (2010). Is visceral fat responsible for the metabolic abnormalities associated with obesity?: implications of omentectomy. *Diabetes Care* **33**, 1693–1694.

Lee YH & Granneman JG (2012). Seeking the source of adipocytes in adult white adipose tissues. *Adipocyte* **1**, 230–236.

Lee YH, Petkova AP, Mottillo EP & Granneman JG (2012). In vivo identification of bipotential adipocyte progenitors recruited by beta3-adrenoceptor activation and high-fat feeding. *Cell Metab* **15**, 480–491.

Lee YS, Kim JW, Osborne O, Oh da Y, Sasik R, Schenk S, Chen A, Chung H, Murphy A, Watkins SM, Quehenberger O, Johnson RS & Olefsky JM (2014). Increased adipocyte O2 consumption triggers HIF-1alpha, causing inflammation and insulin resistance in obesity. *Cell* **157**, 1339–1352.

Lemieux S, Prud'homme D, Bouchard C, Tremblay A & Despres JP (1993). Sex differences in the relation of visceral adipose tissue accumulation to total body fatness. *Am J Clin Nutr* **58**, 463–467.

McCurdy CE, Schenk S, Holliday MJ, Philp A, Houck JA, Patsouris D, MacLean PS, Majka SM, Klemm DJ & Friedman JE (2012). Attenuated Pik3r1 expression prevents insulin resistance and adipose tissue macrophage accumulation in diet-induced obese mice. *Diabetes* **61**, 2495–2505.

Michaud A, Drolet R, Noel S, Paris G & Tchernof A (2012). Visceral fat accumulation is an indicator of adipose tissue macrophage infiltration in women. *Metab Clin Exp* **61**, 689–698.

Modi N, Murgasova D, Ruager-Martin R, Thomas EL, Hyde MJ, Gale C, Santhakumaran S, Dore CJ, Alavi A & Bell JD (2011). The influence of maternal body mass index on infant adiposity and hepatic lipid content. *Pediatr Res* **70**, 287–291.

Ogden CL, Carroll MD, Curtin LR, Lamb MM & Flegal KM (2010). Prevalence of high body mass index in US children and adolescents, 2007–2008. *JAMA* **303**, 242–249.

Okuno A, Tamemoto H, Tobe K, Ueki K, Mori Y, Iwamoto K, Umesono K, Akanuma Y, Fujiwara T, Horikoshi H, Yazaki Y & Kadowaki T (1998). Troglitazone increases the number of small adipocytes without the change of white adipose tissue mass in obese Zucker rats. *J Clin Invest* **101**, 1354–1361.

Parlee SD, Lentz SI, Mori H & MacDougald OA (2014). Quantifying size and number of adipocytes in adipose tissue. *Method Enzymol* **537**, 93–122.

Patel N, Pasupathy D & Poston L (2015). Determining the consequences of maternal obesity for offspring health. *Exp Physiol* **100**, 1421–1428.

Ross R, Berentzen T, Bradshaw AJ, Janssen I, Kahn HS, Katzmarzyk PT, Kuk JL, Seidell JC, Snijder MB, Sorensen TI & Despres JP (2008). Does the relationship between waist circumference, morbidity and mortality depend on measurement protocol for waist circumference? *Obes Rev* **9**, 312–325.

Samuelsson AM, Matthews PA, Argenton M, Christie MR, McConnell JM, Jansen EH, Piersma AH, Ozanne SE, Twinn DF, Remacle C, Rowlerson A, Poston L & Taylor PD (2008). Diet-induced obesity in female mice leads to offspring hyperphagia, adiposity, hypertension, and insulin resistance: a novel murine model of developmental programming. *Hypertension* **51**, 383–392.

Shankar K, Harrell A, Liu X, Gilchrist JM, Ronis MJ & Badger TM (2008). Maternal obesity at conception programs obesity in the offspring. *Am J Physiol Regul Integr Comp Physiol* **294**, R528–R538.

Shasa DR, Odhiambo JF, Long NM, Tuersunjiang N, Nathanielsz PW & Ford SP (2015). Multi-generational impact of maternal overnutrition/obesity in the sheep on the neonatal leptin surge in granddaughters. *Int J Obes (Lond)* **39**, 695–701.

Spalding KL, Arner E, Westermark PO, Bernard S, Buchholz BA, Bergmann O, Blomqvist L, Hoffstedt J, Naslund E, Britton T, Concha H, Hassan M, Ryden M, Frisen J & Arner P (2008). Dynamics of fat cell turnover in humans. *Nature* **453**, 783–787.

Sun K, Kusminski CM & Scherer PE (2011). Adipose tissue remodelling and obesity. *J Clin Invest* **121**, 2094–2101.

Tchkonia T, Morbeck DE, Von Zglinicki T, Van Deursen J, Lustgarten J, Scrable H, Khosla S, Jensen MD & Kirkland JL (2010). Fat tissue, aging, and cellular senescence. *Aging Cell* **9**, 667–684.

Tong JF, Yan X, Zhao JX, Zhu MJ, Nathanielsz PW & Du M (2011). Metformin mitigates the impaired development of skeletal muscle in the offspring of obese mice. *Nutr Diabetes* **1**, e7.

Tost J & Gut IG (2007). DNA methylation analysis by pyrosequencing. *Nat Protoc* **2**, 2265–2275.

van Beek L, van Klinken JB, Pronk AC, van Dam AD, Dirven E, Rensen PC, Koning F, Willems van Dijk K & van Harmelen V (2015). The limited storage capacity of gonadal adipose tissue directs the development of metabolic disorders in male C57Bl/6J mice. *Diabetologia* **58**, 1601–1609.

Vernochet C, Peres SB & Farmer SR (2009). Mechanisms of obesity and related pathologies: transcriptional control of adipose tissue development. *FEBS J* **276**, 5729–5737.

Virtue S & Vidal-Puig A (2010). Adipose tissue expandability, lipotoxicity and the Metabolic Syndrome – an allostatic perspective. *Biochim Biophys Acta* **1801**, 338–349.

Waters TP, Huston-Presley L & Catalano PM (2012). Neonatal body composition according to the revised institute of medicine recommendations for maternal weight gain. *J Clin Endocrinol Metab* **97**, 3648–3654.

White UA & Tchoukalova YD (2014). Sex dimorphism and depot differences in adipose tissue function. *Biochim Biophys Acta* **1842**, 377–392.

Yan X, Zhu MJ, Xu W, Tong JF, Ford SP, Nathanielsz PW & Du M (2010). Up-regulation of Toll-like receptor 4/nuclear factor-kappa B signalling is associated with enhanced adipogenesis and insulin resistance in fetal skeletal muscle of obese sheep at late gestation. *Endocrinology* **151**, 380–387.

Yang QY, Liang JF, Rogers CJ, Zhao JX, Zhu MJ & Du M (2013). Maternal obesity induces epigenetic modifications to facilitate zfp423 expression and enhance adipogenic differentiation in fetal mice. *Diabetes* **62**, 3727–3735.

Yi Z, Stunz LL & Bishop GA (2014). CD40-mediated maintenance of immune homeostasis in the adipose tissue microenvironment. *Diabetes* **63**, 2751–2760.

Zeve D, Tang W & Graff J (2009). Fighting fat with fat: the expanding field of adipose stem cells. *Cell Stem Cell* **5**, 472–481.

Additional information

Competing interests

The authors declare that they have no competing interests.

Author contributions

XL, QY, XF, CJR, BW, HP and MD researched the data and wrote the manuscript. MJZ and PWN contributed to the experimental design and discussion and reviewed and edited the manuscript. MD designed the experiments. All the experiments were performed in Washington State University, except for the cell sorting with flow cytometry, which was carried out in University of Idaho. All authors have approved the final version of the manuscript. All authors agree to be accountable for all aspects of the work, ensuring that questions related to the accuracy or integrity of any part are appropriately investigated and resolved. All persons designated as authors qualify for authorship, and all those who qualify for authorship are listed.

Funding

The present study was funded by NIH R01HD067449.

Acknowledgements

The authors wish to thank Ann Norton for performing the cell sorting with flow cytometry.